

Analysis of effect of annealing at high temperature on nickel oxide and zinc oxide thin film for solar cell applications

Iskandar Dzulkarnain Rummaja¹, Nur Afiqah Hani Senin¹, Muhammad Idzdihar Idris^{1,2},
Zarina Baharudin Zamani¹, Radi Husin Ramlee¹, Luke Bradley³

¹Faculty of Electronic and Computer Technology and Engineering, Universiti Teknikal Malaysia Melaka (UTeM), Melaka, Malaysia

²Micro and Nano Electronic Research Group (MiNE), Faculty of Electronic and Computer Technology and Engineering,
Universiti Teknikal Malaysia Melaka (UTeM), Melaka, Malaysia

³Cyro-Electronics at School of Engineering, Newcastle University, Newcastle upon Tyne, United Kingdom

Article Info

Article history:

Received Nov 27, 2023

Revised Jan 23, 2024

Accepted Jan 25, 2024

Keywords:

Annealing

Characterization

So-gel

Spin coat deposition

Thin film

ABSTRACT

The use of thin films in solar cell technology has gained substantial interest because of their potential for cost-effective and efficient energy conversion. nickel oxide (NiO) and zinc oxide (ZnO) have been used as potential materials in solar cells application especially third generation solar cells because of their good characteristics, such as high electrical conductivity, chemical stability, resistance to degradation, and abundance and low cost. However, at high temperatures, both NiO and ZnO can undergo thermal decomposition and exhibit crystal defects and grain boundaries. This work investigates high temperature annealing on the morphology, structural, and optical properties of NiO and ZnO thin films. The deposited material was annealed at 500 °C, 600 °C, and 700 °C and be characterized via scanning electron microscopy (SEM), XRD, and UV-Vi's spectroscopy. The results showed that increasing the annealing temperature can improve both ZnO and NiO thin films in structure and appearance. For ZnO, higher temperatures made the grains bigger and more orderly, and for NiO, the process made the grains more organized, bigger in size, and spread out more evenly. However, annealing at high temperature yields a smaller bandgap energy value for both thin films.

This is an open access article under the [CC BY-SA](https://creativecommons.org/licenses/by-sa/4.0/) license.



Corresponding Author:

Muhammad Idzdihar Idris

Faculty of Electronic and Computer Technology and Engineering

Universiti Teknikal Malaysia Melaka (UTeM)

Hang Tuah Jaya, 76100 Durian Tunggal, Melaka, Malaysia

Email: idzdihar@utem.edu.my

1. INTRODUCTION

The quest for sustainable and renewable sources of energy has led to remarkable advancements in the field of photovoltaics, with solar cells emerging as a prominent solution for harnessing solar energy. Among the various generations of solar cells, third-generation solar cells have garnered substantial attention due to their potential to enhance the efficiency and cost-effectiveness of solar energy conversion. This class of solar cells encompasses a range of innovative technologies, including dye-sensitized solar cells (DSSCs) and perovskite solar cells (PSC), quantum dot sensitized solar cells (QDSSC), tandem solar cells, and organic solar cells (OPV) [1] which are distinguished by their utilization of novel materials in their component design.

Nickel oxide (NiO), an extensively researched p-type transition metal oxides, is characterized by its economical cost, non-toxic nature, and optical transparency. Its bandgap exhibits a significant range, shifting

from 3.6 eV to 4.0 eV [2]. Notably, modifications in precursors, diverse preparation techniques, and variations in doping concentrations can all influence these bandgap values [3]. NiO possesses an octahedral structure, with nickel (Ni) in a (II) oxidation state and oxygen ions (O^{2-}) akin to the arrangement found in sodium chloride (NaCl). NiO has a cubic crystal structure at temperatures above the Néel temperature (523 K). However, when the temperature drops below this point, the crystal structure slightly distorts, forming a rhombohedral configuration associated with anti-ferromagnetic behavior. The distinctive structural characteristic of NiO has made NiO a subject of great interest among researchers, primarily due to its wide-ranging applicability in fields such as anti-ferromagnetic materials, chemical sensors, electrochromic devices, catalysts, and solar cell. NiO has been extensively explored and used as a constituent material in solar cell applications, particularly in third-generation solar cells. NiO emerges as a promising candidate for the role of counter electrode in DSSCs due to its powerful interaction with ions from iodine-based electrolytes, resulting in excellent catalytic activity [4].

Feihl *et al.* [5] investigated NiO thin films as counter electrodes, discovering favourable properties such as homogeneity, transparency, and efficient light harvesting, in addition to noteworthy conductivity. Chen *et al.* [6] proposed doping NiO with phosphorous as a counter electrode for DSSCs in order to improve NiO's catalytic capabilities. This change yielded an exceptional power conversion efficiency (PCE) of 9.05%. NiO is used in perovskite solar cells as a promising hole transfer material (HTM) in addition to DSSCs. NiO is well-suited for this job due to its remarkable properties such as high hole mobility, electrical conductivity, transmittance, energetically favourable band alignment, and environmental stability [7]. Yin *et al.* [8] employed a straightforward process to create NiO thin films as HTMs in perovskite solar cells, achieving a peak power conversion efficiency of 15.71% with a thin film thickness of 59 nm. Shanna *et al.* [9] also investigated NiO's performance as an HTM in inverted perovskite solar cells. They achieved a remarkable power conversion efficiency of 22.95% by optimising $CH_3NH_3SnI_3$ as the absorber layer utilising SCAPS software simulations [9].

Zinc oxide (ZnO) stands out as a readily accessible and economical semiconductor material renowned for its non-toxic properties and widespread availability. This semiconductor possesses distinctive traits, including n-type conductivity and a spacious energy band gap, registering at 3.37 eV under room temperature conditions [10], [11]. Notably, ZnO exhibits a significant excitonic binding energy of up to 60 meV. Additionally, it showcases impressive optical characteristics, boasting high transmittance that surpasses 80% within the visible spectrum. Simultaneously, when adequately doped, ZnO displays low electrical resistivity [12]. ZnO has a unique combination of potentially exciting features, including high bulk electron mobility and possibly the most diversified array of nanostructures available via a wide range of production methods. Taking use of these properties, ZnO has found use as a photoanode material in DSSC [13], [14]. Sufyan *et al.* [15] used a hydrothermal technique to synthesise ZnO nanorods, which they used as a photoanode in DSSC and achieved an efficiency of 2.08%. This performance outperforms that of traditional DSSCs based on ZnO nanoparticles, which achieve a 1.19% efficiency.

Furthermore, because of its high electron mobility and high transparency, ZnO emerges as an attractive contender for usage as an electron transport layer (ETL) in perovskite solar cells [15]. Zheng *et al.* used combustion synthesis to create a ZnO thin film for use as an ETL in perovskite solar cells, with a focus on low-temperature production. Their method produced high-quality ZnO films with exceptional crystallinity, resulting in an impressive power conversion efficiency (PCE) of 20% [16]. In addition, ZnO has been employed as a photoanode in quantum dot sensitised solar cells (QDSSC). Raj *et al.* [17] proposed using a single-crystalline ZnO nanorod array to make CdSe/CdS/PbS/ZnO quantum dot sensitised solar cells (QDSSC). Their findings demonstrated improved short-circuit density, resulting in a PCE of 2.35%.

Annealing is a critical stage in the fabrication of thin films, including the application of heat to the deposited thin film at a certain temperature and duration. Annealing is used to crystallise the deposited thin film, improving its structural order and electrical characteristics. Tatyana *et al.* [19] used the Sol-Gel method to successfully fabricate a NiO thin film. The deposited thin film was annealed at increasingly higher temperatures at 200 °C, 300 °C, 400 °C, and 500 °C [18]. The study focused on the effect of annealing at various temperatures ranging from low (200 °C) to high (500 °C). As a result, x-ray photoelectron spectroscopy (XPS) study confirmed the production of NiO with the presence of Ni⁺ states during 400 °C annealing. After treatment at 200 °C, the films initially displayed high optical transparency, reaching 90% in the visible range. However, after 500 °C high-temperature annealing, this transparency decreased to 76-78%. During heat treatment, the optical band gap of the NiO_x films reduced, ranging from 3.92 to 3.68 eV. This result demonstrates a decrease in optical transparency as the annealing temperature rises. Furthermore, Toe *et al.* [20] have investigated the effect of low-temperature annealing on the performance of ZnO. The ZnO thin films were annealed for 60 minutes at 350 °C, 450 °C, 550 °C, and 650 °C. The observations demonstrated an increase in crystal grain size with increasing annealing temperature, which was attributed to

the Ostwald ripening phenomenon. Furthermore, higher temperatures aided in the adherence of thin films to the FTO glass substrate, resulting in an increase in ZnO production.

In this work, the effects of annealing at high temperatures (500 °C to 700 °C) on NiO and ZnO thin films were thoroughly investigated. The NiO thin films were prepared using the sol-gel method, and then the ZnO and NiO thin films were deposited to the FTO glass by spin-coating. Subsequently, characterisation techniques were employed to evaluate the thin films' surface characteristics, morphological characteristics, and structural integrity. This methodical approach provides important insights into optimising the properties of the thin film as component of solar cells.

2. METHOD

2.1. Preparation of nickel oxide precursor

The NiO precursor was created using the sol-gel technique [19]. Initially, 0.622 g of nickel acetate tetrahydrate ($C_4H_{14}NiO_8$) was dissolved in 10 ml of ethanol (C_2H_5OH) and 15 ml of isopropyl alcohol (IPA) in the first step. Stirring was continued until full dissolution was accomplished. To keep the pH of the solution at 10 [20], potassium hydroxide (KOH) was added dropwise. Following that, the solution was stirred for 2 hours on a hot plate set at 60 °C. The resulting mixture was centrifuged, resulting in the separation of a supernatant and a precipitate. The resulting precipitate was rinsed with ethanol five times to remove any leftover compounds before drying at 60 °C for one hour. This procedure resulted in the formation of a green gel. Figure 1 provides an illustrative depiction of the step-by-step preparation procedure for NiO via the sol-gel method.

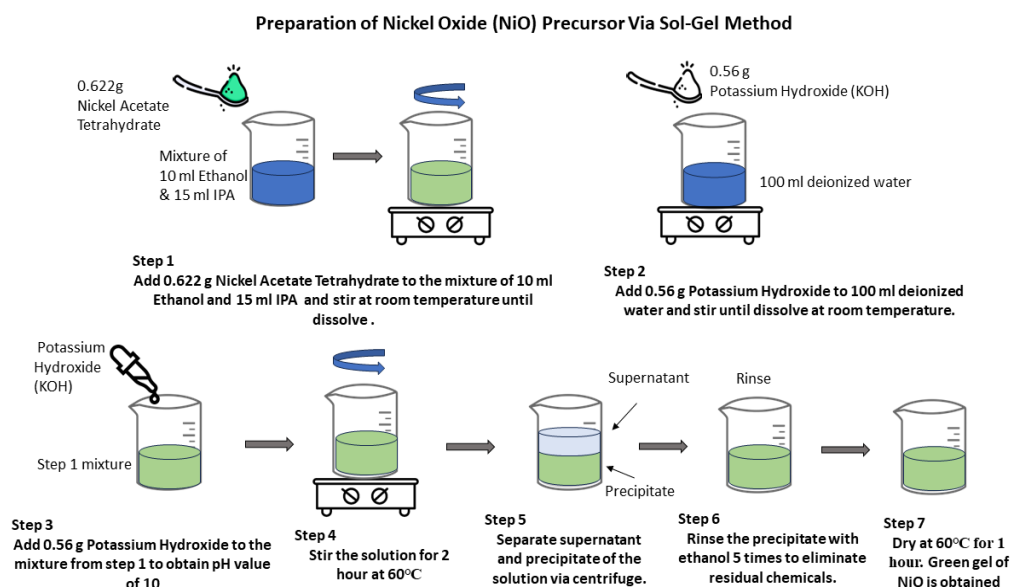


Figure 1. Illustration of the preparation procedure of NiO via sol-gel method

2.2. Preparation of ZnO paste

The binder consists of 19g α -terpineol [Sigma-Aldrich], and 1g of ethyl cellulose was purchased from sigma-aldrich, supplied from Merck (Darmstadt, Germany). The resultant was stirred for 24h on a hot plate to ensure the solution mixed well. ZnO nanoparticles were purchased from sigma aldrich (<100 nm, 20 wt. % in H₂O) combined with a binder with 35% and 65% ratios, respectively. The combined solution was stirred for 24h on a hot plate at 200 rpm.

2.3. Preparation of NiO and ZnO thin film

The spin coating technique was used to create NiO and ZnO thin films, as shown in Figure 2. The solution was dispensed over a clean glass substrate (Microscope glass). Following that, the NiO and ZnO substrates were spin-coated for 30 seconds at 3,000 rpm and 50 seconds at 3,000 rpm, respectively. The thin films were dried at 150 °C for 15 minutes to remove organic residuals. For NiO thin films, this spin coating and drying process was repeated 10 times, while for ZnO thin films, it was repeated once. The resulting thin films were annealed in a furnace at three different temperatures (500 °C, 600 °C, and 700 °C). Table 1 summarises the deposition parameters for NiO and ZnO thin films.

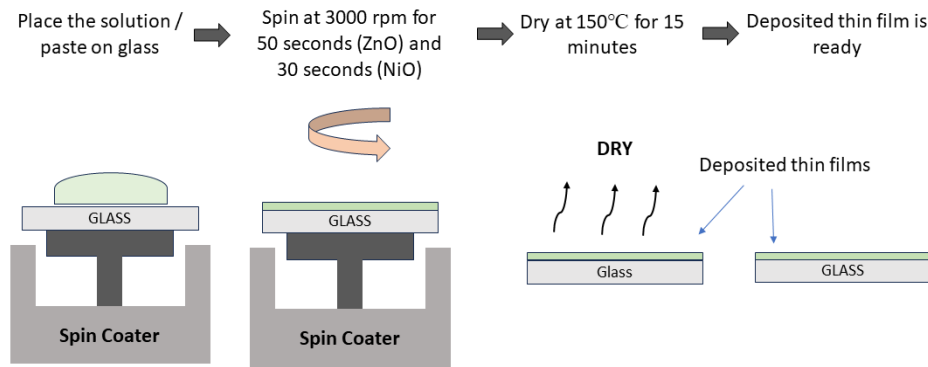


Figure 2. Procedure of deposition via spin coating method

Table 1. Summary deposition of NiO and ZnO thin film

Sample	Temperature	Speed/Time
NiO	As deposited	3,000 rpm/30 seconds
	500 °C	
	600 °C	
	700 °C	
ZnO	As deposited	3,000 rpm/50 seconds
	500 °C	
	600 °C	
	700 °C	

2.4. Characterization of NiO and ZnO thin film

The characterization of ZnO and NiO thin films was conducted through x-ray diffraction (XRD), scanning electron microscopy (SEM), and UV-visible spectroscopy analyses. XRD (PANalytical XPert PRO) was utilized to assess the crystallinity of the films with a wavelength of 0.154 nm. For investigating the surface morphology, field emission scanning microscopy (SEM, Zeiss EVO 50) was employed. Lastly, UV-visible spectroscopy (Shimadzu UV-1800) was employed to determine the optical characteristics. The optical band gap energy was calculated using in (1) and (2), based on the Tauc relation for direct bandgap materials [21].

$$(\alpha hv)^2 = A (hv - E_g) \quad (1)$$

$$\alpha = 2.303 A/t \quad (2)$$

3. RESULTS AND DISCUSSION

3.1. Characterization of NiO thin film

3.1.1. XRD analysis of NiO thin films

The grazing mode of XRD was used to explore the structural properties of the thin films, and intensity data were collected within a 2θ range of 30° to 80° . The XRD patterns of NiO thin films subjected to varied annealing temperatures (as-deposited, 500°C , 600°C , and 700°C) are shown in Figure 3. The NiO film showed two prominent peaks at 37.3° and 63.01° in the pattern corresponding to pH 10 after annealing. These peaks correspond to the (1 1 1) and (2 2 0) cubic NiO diffraction planes, respectively, as confirmed by the international centre for diffraction data (ICDD 00-044-1159) [22]. Based on the XRD pattern, it was observed that the highest peak was at 600°C . The XRD pattern shows two peaks at annealing temperature of 600°C and 700°C . The results are similar as reported by previous works [23]–[25] with two peaks available in the XRD pattern.

3.1.2. UV-VIS analysis of NiO thin films

To investigate the optical absorption spectra of NiO thin films with different annealing temperatures and analyze the energy bandgap, UV-Visible analysis was used in Figure 4. Figure 4(a) depicts the wavelength dependence of absorption in the spectral region 295–800 nm for NiO thin films. Due to the energy gap created by the NiO thin films, the absorbance decreased rapidly at short wavelengths. As a result, there is an absorption peak at 295 nm for NiO at annealed temperatures of 500° and 700°C . These results are

almost similar to previous papers [26], [27]. The highest absorption was annealed temperature at 700° due to the high crystallinity. Annealing at this temperature diffused and reorganized the NiO's atoms into a more ordered crystalline structure. Higher crystallinity allows the material to absorb and convert incident light into electrical energy, increasing absorption.

Figure 4(b) shows the absorption coefficient in same wavelength. The absorption coefficient can be calculated using in (4), which t represents the thickness of the sample and A is the absorbance. On the other hand, the highest absorption coefficient of NiO thin films annealed at 500 °C at peak $2 \times 10^6 \text{ cm}^{-1}$ and decreased at annealed temperatures of 600 °C and 700 °C, as indicated in Figure 4(b). These results have a good agreement with previous work [28].

The optical energy band gap (E_g) is calculated using the classical relationship shown in (1). The value of n in the equals (2) for allowed indirect optical transitions. This work determined the indirect bandgap by plotting a graph between $(\alpha h\nu)^2$ and $(h\nu)$ in eV, as indicated in Figure 5. The band gap values were obtained with different annealing temperatures are 4.10 eV, 3.50 eV, 3.43 eV, and 3.59 eV for as deposited, 500 °C, 600 °C, and 700 °C, respectively. Furthermore, these findings are almost same with the findings of the researchers [22] as the researchers obtained the result of 3.86 eV, 3.69 eV, 3.60 eV, and 3.47 eV for same varied temperature in this work.

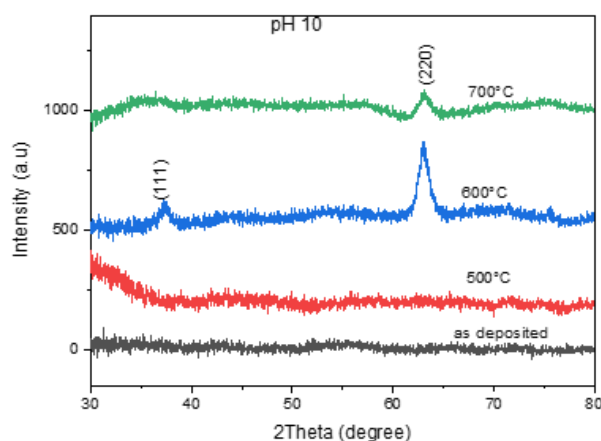


Figure 3. XRD patterns illustrating NiO thin films at various annealing temperatures

3.1.3. SEM images analysis of NiO thin films

Surface morphology analysis of NiO thin films annealed at different temperatures (500 °C, 600 °C, and 700 °C) was conducted using SEM. The surface morphology of NiO can change with increasing temperature because of several factors, including changes in crystal structure, surface diffusion rates, and surface oxidation/reduction reactions. Figure 6 shows the SEM image of NiO with the magnification of 10,000 obtained by focusing the electron beam over the surface of the sample to generate the 2-dimensional images. As shown in the micrographs, top views of the NiO films reveal nanocrystalline grains that uniformly cover the substrate's surface. The NiO thin films show smooth and homogenous surfaces for NiO thin films as deposited and 500 °C, as indicated in Figure 6(b). As shown in the micrographs, top views of the NiO films reveal nanocrystalline grains that uniformly cover the substrate's surface. The micrography results clearly reveal that the nanoparticles are extremely fine and uniformly distributed across the glass substrate. These results reported similar SEM images for NiO thin films with previous works where the NiO thin films show smooth and homogenous surfaces due to the changes in surface morphology that occur with increasing temperature [29], [30].

3.2. Characterization of ZnO thin films

3.2.1 XRD analysis of ZnO thin films

The same XRD technique used for the NiO thin film was used for the structural study of the ZnO thin film. Data on intensity were collected throughout a two-degree range of 20° to 80°. The XRD pattern of ZnO thin films at various annealing temperatures is shown in Figure 7. The major peaks of the ZnO films align with the indices (100), (002), and (101), which are located at 31.67°, 34.47°, and 36.18°, respectively, across all samples. Surprisingly, the (101) plane had the highest intensity in all samples except those annealed at 700 °C [21]. With increasing annealing, it was expected that the intensity of the peaks would increase. Nevertheless, the peaks observed in the sample annealed at 700 °C were notably smaller in

comparison to those of the other samples. This discrepancy could be attributed to the diminished durability of the glass substrate, which exhibited signs of melting at around 700 °C. The XRD analysis revealed that all the ZnO thin film samples exhibited the characteristic XRD pattern of ZnO, aligning well with findings from previously reported studies [31]–[33].

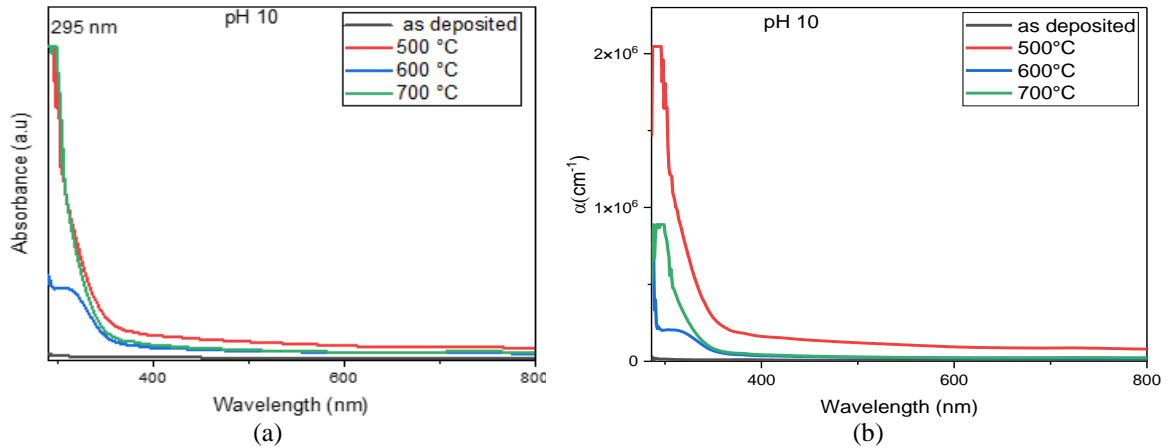


Figure 4. Ultraviolet-visible (UV-vis) spectra of NiO at varying annealing temperatures (a) UV-Vi's absorption of NiO and (b) Absorption coefficient of NiO

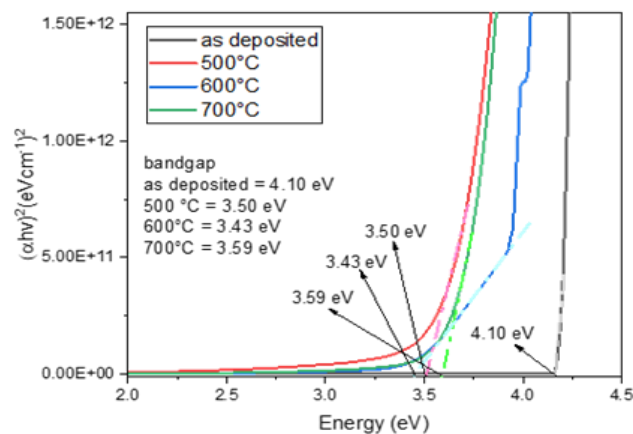


Figure 5. Optical band gap of NiO thin films

3.2.2. UV-VIS of ZnO thin films

The absorbance of ZnO thin films at various annealing temperatures was investigated using UV-visible analysis. From Figure 8(a), the absorption peak position with different annealing temperatures is 372 nm, 363 nm, and 343 nm for 500 °C, 600 °C, and 700 °C, respectively. These results are in the range reported by previous work [34], [35]. The ZnO thin film annealed at 500 °C exhibited the highest spectrum along the wavelength. The absorption spectra of other samples decreased with the increasing annealing temperatures because the particle size grew, and the sample dispersion degraded at the highest temperature [36]. In addition, as the annealing temperature increases, the band gap of the thin film also increases. A larger band gap results in lower absorbance, as it requires more energy for the material to absorb light, reducing its ability to interact with the surrounding environment [37].

The plot of $(\alpha h\nu)^2$ vs. $h\nu$ indicated in Figure 8(b) shows that ZnO has band gaps of 4.17 eV, 3.94 eV, and 3.85 eV with annealing temperatures at 500 °C, 600 °C, and 700 °C, respectively. However, these results contradicted previous work [22], [23], [38], and the optical bandgap obtained was higher than bulk ZnO 3.37 eV [25].

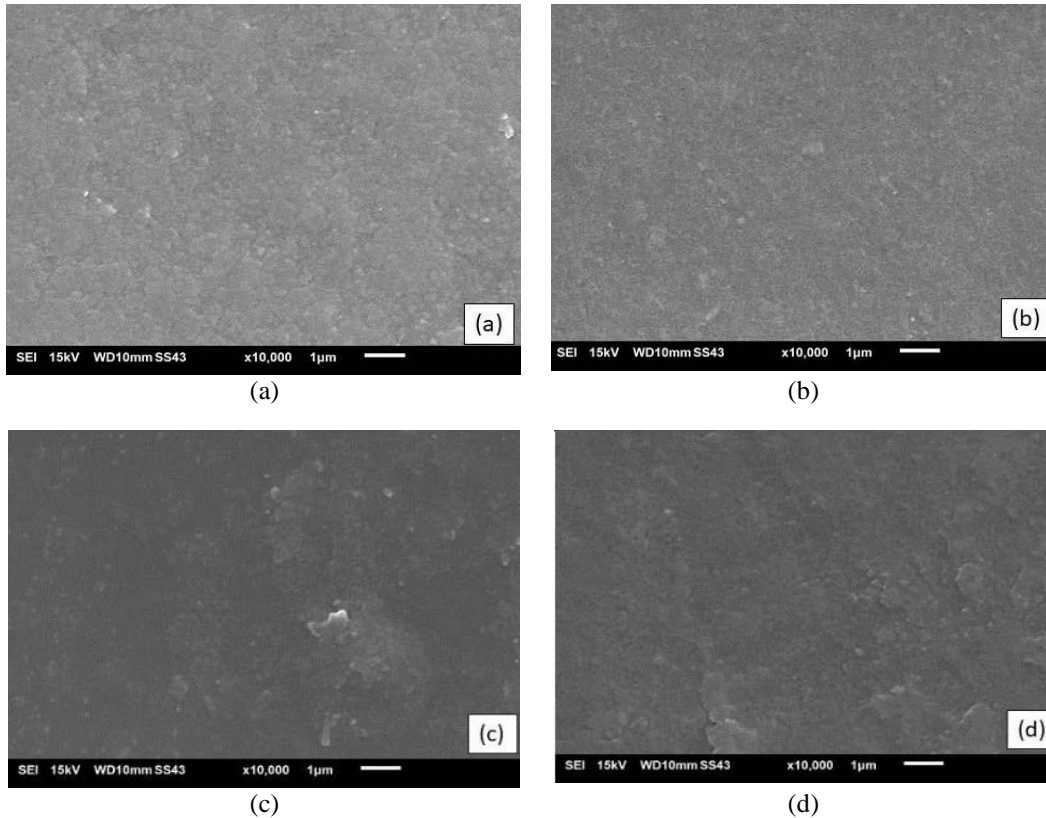


Figure 6. SEM images of NiO thin film subjected to varying annealing temperatures; (a) as deposited, (b) 500 °C, (c) 600 °C, and (d) 700 °C

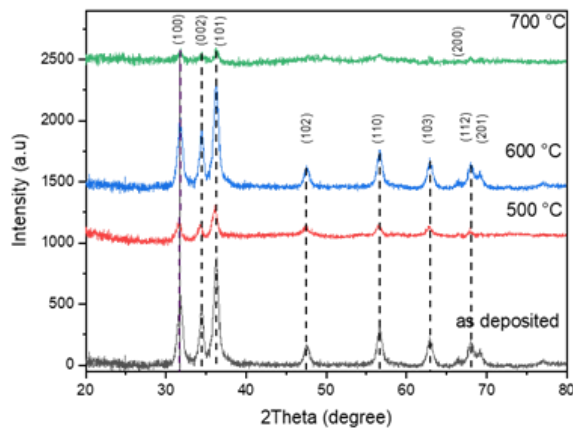


Figure 7. XRD spectra depicting ZnO thin films at various annealing temperatures (as deposited 500 °C, 600 °C, and 700 °C)

3.2.3. SEM analysis of ZnO thin films

SEM images of ZnO thin films at magnifications of 5,000 for samples 500 °C, 600 °C, and 700 °C are shown in Figure 9. Figure 9(a) for the ZnO thin film samples annealed at 500 °C reveals that the particles are distributed equally and that their attachment to one another results in agglomerated particles. These results for ZnO annealed at 500 °C were almost the same as reported by previous work [31], where the ZnO particles formed very uniformly. In addition, the grain size of ZnO thin films was obtained in the range of 0.20-0.40 μm. The average grain size was measured using ImageJ software. Figure 9(b) reveals the increasing grain size at 0.41 μm from 0.29 μm when the sample annealed at 600 °C. Figure 9(c) shows the image after annealing at 700 °C because of the low durability of glass. As a result, only the binder was presented when SEM was conducted.

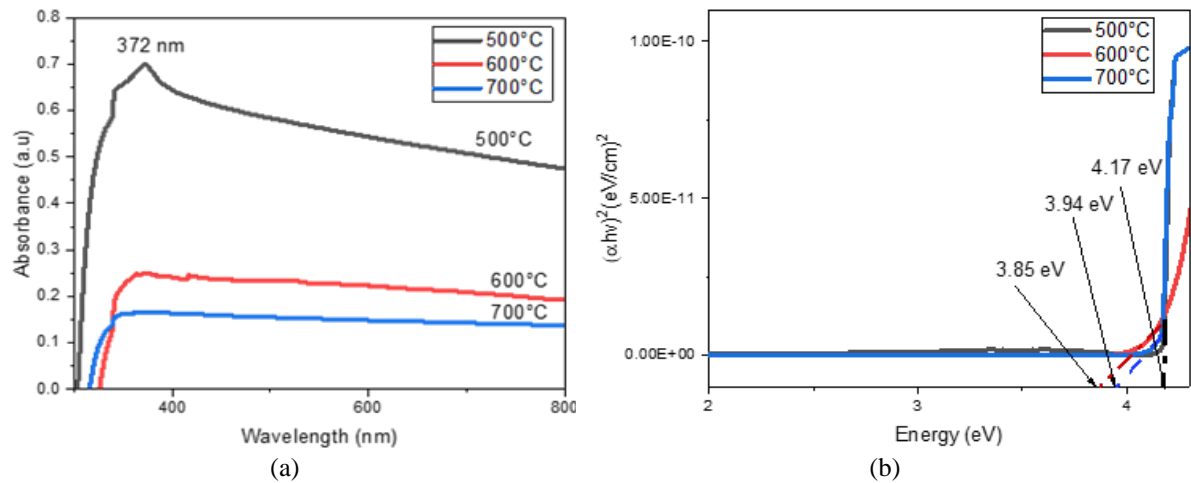


Figure 8. UV Vis and bandgap of ZnO thin film (a) UV-Vis absorption spectrum of ZnO thin films at different annealing temperatures and (b) the optical bandgap of ZnO at different annealing temperatures

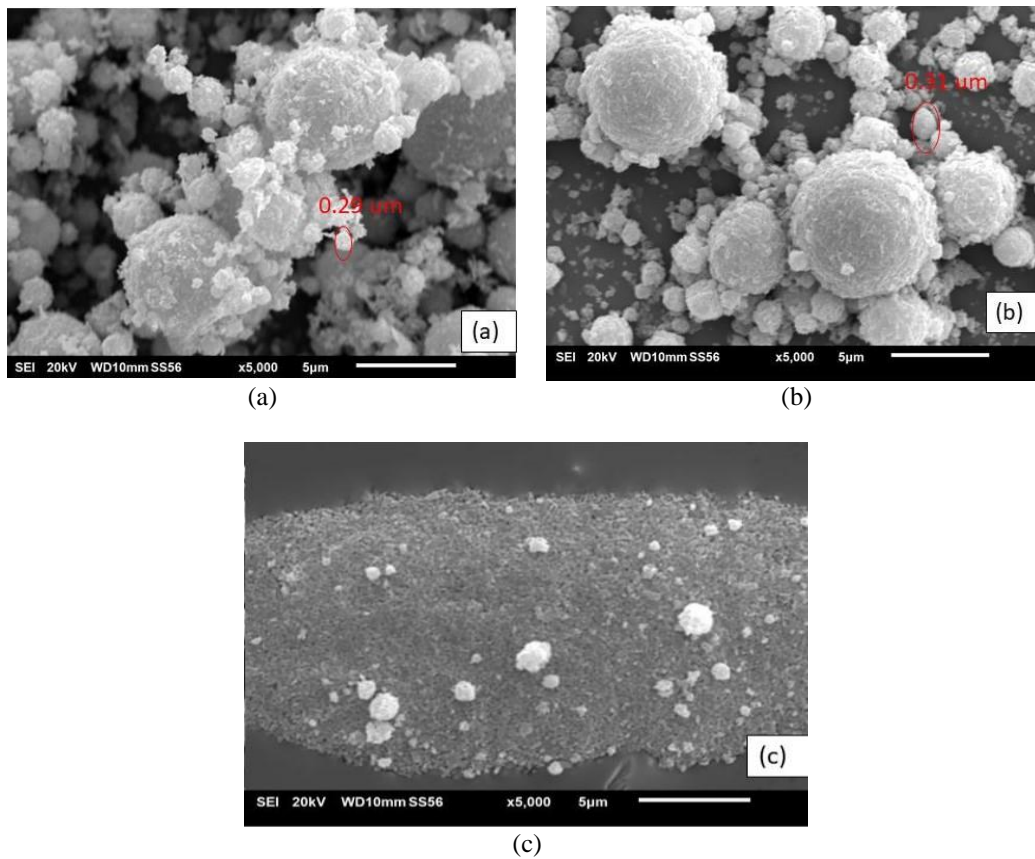


Figure 9. SEM images showing ZnO thin films at different annealing temperatures; (a) 500 °C, (b) 600 °C, and (c) 700 °C

4. CONCLUSION

The conclusion of the study on the effect of annealing temperature on the deposition of ZnO and NiO thin films is that increasing the annealing temperature can improve the structural and morphological properties of both ZnO and NiO thin films. For NiO, the annealing process improved crystallinity, increased particle size, and more uniform distribution especially at 700 °C. However, bandgap energy decreased when

the thin film was annealed from 4.10 eV into 3.50 eV, 3.43 eV, and 3.59 eV. The result of UV Vis analysis shows that the annealing at high temperatures showing decreasing bandgap energy trends in both of thin films. XRD analysis of NiO shows that annealing at high temperature resulted in the increase of crystallite size and enhancement of the intensity of the (111) reflection. For ZnO, annealing at higher temperatures resulted in larger and more ordered grains from 0.29 μm at 500 °C and 0.41 μm at 600 °C, but at 700 °C, there no ZnO present on the film but only binder is presented. In addition, at higher annealing temperatures, the absorption spectra had sharper peaks, which indicated a uniform crystalline structure. However, the absorption band edge shifted to a shorter wavelength, indicating smaller bandgap energy at 3.85 eV. Moreover, XRD analysis of ZnO films show the diffraction peak corresponding to the (002) planes became sharper and shifted to a higher degree with the increase in annealing temperature, indicating enhanced crystal orientation along the c-axis and reduction in lattice strain. In addition, the XRD analyses of the ZnO and NiO films indicate that heightened annealing temperatures result in an enhanced structural integrity and crystalline nature for both materials.

ACKNOWLEDGEMENTS

This work was supported by the Ministry of Higher Education Malaysia and Universiti Teknikal Malaysia Melaka (UTeM) through Project No PJP/2021/FKEKK/S01820.





REFERENCES

- [1] N. Shah *et al.*, "A review of third generation solar cells," *Processes*, vol. 11, no. 6, p. 1852, Jun. 2023, doi: 10.3390/pr11061852.
- [2] S. Maitra, S. Pal, S. Datta, T. Maitra, B. Dutta, and S. Roy, "Nickel doped molybdenum oxide thin film counter electrodes as a low-cost replacement for platinum in dye sensitized solar cells," *Materials Today: Proceedings*, vol. 39, pp. 1856–1861, 2021, doi: 10.1016/j.matpr.2020.07.531.
- [3] S. Muniandy, M. I. Idris, Z. A. F. M. Napiah, H. H. M. Yusof, S. A. M. Chachuli, and M. Rashid, "An investigation on NiO for hole transport material in perovskite solar cells," in *2021 IEEE Regional Symposium on Micro and Nanoelectronics (RSM)*, IEEE, Aug. 2021, pp. 112–115. doi: 10.1109/RSM52397.2021.9511573.
- [4] H. Wang, W. Wei, and Y. H. Hu, "NiO as an efficient counter electrode catalyst for dye-sensitized solar cells," *Top Catal*, vol. 57, no. 6–9, pp. 607–611, Apr. 2014, doi: 10.1007/s11244-013-0218-8.
- [5] S. Feihl *et al.*, "Nickel oxide nanostructured electrodes towards peryleneimide-based dye-sensitized solar cells," *RSC Advances*, vol. 2, no. 30, p. 11495, 2012, doi: 10.1039/c2ra22206j.
- [6] Y.-L. Chen *et al.*, "Nanoflower-like P-doped nickel oxide as a catalytic counter electrode for dye-sensitized solar cells," *Nanomaterials*, vol. 12, no. 22, p. 4036, Nov. 2022, doi: 10.3390/nano12224036.
- [7] H. Park, R. Chaurasiya, B. H. Jeong, P. Sakthivel, and H. J. Park, "Nickel oxide for perovskite photovoltaic cells," *Advanced Photonics Research*, vol. 2, no. 8, Aug. 2021, doi: 10.1002/adpr.202000178.
- [8] X. Yin *et al.*, "High efficiency inverted planar perovskite solar cells with solution-processed NiO x hole contact," *ACS Applied Materials & Interfaces*, vol. 9, no. 3, pp. 2439–2448, Jan. 2017, doi: 10.1021/acsami.6b13372.
- [9] M. S. Shamna, K. S. Nithya, and K. S. Sudheer, "Simulation and optimization of CH₃NH₃SnI₃ based inverted perovskite solar cell with NiO as hole transport material," *Materials Today: Proceedings*, vol. 33, pp. 1246–1251, 2020, doi: 10.1016/j.matpr.2020.03.488.
- [10] S. S. Parui, N. Kumar, P. Tiwari, N. Tiwari, and R. N. Chauhan, "Zinc oxide and cupric oxide based thin films for solar cell applications," *Materials Today: Proceedings*, vol. 41, pp. 233–236, 2021, doi: 10.1016/j.matpr.2020.08.799.
- [11] S. Muhammad, A. T. Nomaan, M. I. Idris, and M. Rashid, "Structural, optical and electrical investigation of low-temperature processed zinc oxide quantum dots based thin films using precipitation-spin coating on flexible substrates," *Physica B: Condensed Matter*, vol. 635, p. 413806, Jun. 2022, doi: 10.1016/j.physb.2022.413806.
- [12] S. Mridha and D. Basak, "Investigation of a p-CuO/n-ZnO thin film heterojunction for H₂ gas-sensor applications," *Semiconductor Science and Technology*, vol. 21, no. 7, pp. 928–932, Jul. 2006, doi: 10.1088/0268-1242/21/7/017.
- [13] J. A. Anta, E. Guillén, and R. Tena-Zaera, "ZnO-based dye-sensitized solar cells," *The Journal of Physical Chemistry C*, vol. 116, no. 21, pp. 11413–11425, May 2012, doi: 10.1021/jp3010025.
- [14] M. I. Idris, H. H. M Yusof, Z. A. F. M. Napiah, M. Rashid, M. N. S. Zainudin, and H. Zainuddin, "The effect of seeding method on the growth of zinc oxide nanorods," *International Journal of Nanoelectronics & Materials*, 2023.
- [15] M. Sufyan, U. Mehmood, Y. Qayyum Gill, R. Nazar, and A. Ul Haq Khan, "Hydrothermally synthesize zinc oxide (ZnO) nanorods as an effective photoanode material for third-generation Dye-sensitized solar cells (DSSCs)," *Mater Lett*, vol. 297, p. 130017, Aug. 2021, doi: 10.1016/j.matlet.2021.130017.
- [16] C. Qiu, Y. Wu, J. Song, W. Wang, and Z. Li, "Efficient planar perovskite solar cells with ZnO electron transport layer," *Coatings*, vol. 12, no. 12, p. 1981, Dec. 2022, doi: 10.3390/coatings12121981.
- [17] D. Zheng *et al.*, "Combustion synthesized zinc oxide electron-transport layers for efficient and stable perovskite solar cells," *Advanced Functional Materials*, vol. 29, no. 16, Apr. 2019, doi: 10.1002/adfm.201900265.
- [18] C. Justin Raj *et al.*, "Improved photovoltaic performance of CdSe/CdS/PbS quantum dot sensitized ZnO nanorod array solar cell," *J Power Sources*, vol. 248, pp. 439–446, Feb. 2014, doi: 10.1016/j.jpowsour.2013.09.076.
- [19] T. Ivanova, A. Harizanova, M. Shipochka, and P. Vitanov, "Nickel oxide films deposited by sol-gel method: effect of annealing temperature on structural, optical, and electrical properties," *Materials*, vol. 15, no. 5, p. 1742, Feb. 2022, doi: 10.3390/ma15051742.
- [20] M. Z. Toe, A. Matsuda, S. S. Han, K. A. Yaacob, and S.-Y. Pung, "Effect of annealing temperature on the performance of ZnO thin film-based dye sensitized solar cell," 2020, p. 020010. doi: 10.1063/5.0015699
- [21] S. Muniandy, M. I. Idris, Z. A. F. M. Napiah, and M. Rashid, "The effect of pH level and annealing temperature on NiO thin films as hole transport material in inverted perovskite solar cells," in *2022 IEEE International Conference on Semiconductor Electronics (ICSE)*, IEEE, Aug. 2022, pp. 13–16. doi: 10.1109/ICSE56004.2022.9863126.




- [22] S. Muniandy *et al.*, “The effect of different precursor solutions on the structural, morphological, and optical properties of nickel oxide as an efficient hole transport layer for perovskite solar cells,” *Pertanika Journal of Science & Technology*, vol. 31, no. 4, pp. 2047–2066, Jul. 2023, doi: 10.47836/pjst.31.4.26.
- [23] D. Raoufi, “Synthesis and photoluminescence characterization of ZnO nanoparticles,” *Journal of Luminescence*, vol. 134, pp. 213–219, Feb. 2013, doi: 10.1016/j.jlumin.2012.08.045.
- [24] V. P. Patil *et al.*, “Effect of annealing on structural, morphological, electrical and optical studies of nickel oxide thin films,” *Journal of Surface Engineered Materials and Advanced Technology*, vol. 01, no. 02, pp. 35–41, 2011, doi: 10.4236/jsemat.2011.12006.
- [25] N. A. Bakr, S. A. Salman, and A. M. Shano, “Effect of co doping on structural and optical properties of NiO thin films prepared by chemical spray pyrolysis method,” *International Letters of Chemistry, Physics and Astronomy*, vol. 41, pp. 15–30, Nov. 2014, doi: 10.18052/www.scipress.com/ILCPA.41.15.
- [26] P. Ravikumar, D. Taparia, and P. Alagarsamy, “Thickness-dependent thermal oxidation of Ni into NiO thin films,” *Journal of Superconductivity and Novel Magnetism*, vol. 31, no. 11, pp. 3761–3775, Nov. 2018, doi: 10.1007/s10948-018-4651-6.
- [27] C.-C. Diao, C.-Y. Huang, C.-F. Yang, and C.-C. Wu, “Morphological, optical, and electrical properties of p-type nickel oxide thin films by nonvacuum deposition,” *Nanomaterials*, vol. 10, no. 4, p. 636, Mar. 2020, doi: 10.3390/nano10040636.
- [28] A. Diallo *et al.*, “Structural, optical and photocatalytic applications of biosynthesized NiO nanocrystals,” *Green Chemistry Letters and Reviews*, vol. 11, no. 2, pp. 166–175, Apr. 2018, doi: 10.1080/17518253.2018.1447604.
- [29] K. M. Racik, M. Joseph, M. K. Racik, J. Madhavan, and M. V. A. Raj, “Synthesis, characterization and optical properties of spherical NiO nanoparticles preparation and optical properties of cadmium oxide semiconductor nanoparticles view project synthesis, characterization and optical properties of spherical NiO nanoparticles,” *Researchgate*, 2018. [Online]. Available: <https://www.researchgate.net/publication/331928066>
- [30] M. Ono *et al.*, “Relation between electrical and optical properties of p-type NiO films,” *physica status solidi (b)*, vol. 255, no. 4, p. 1700311, Apr. 2018, doi: 10.1002/pssb.201700311.
- [31] A. A. Al-Ghamdi, W. E. Mahmoud, S. J. Yagmour, and F. M. Al-Marzouki, “Structure and optical properties of nanocrystalline NiO thin film synthesized by sol–gel spin-coating method,” *Journal of Alloys and Compounds*, vol. 486, no. 1–2, pp. 9–13, Nov. 2009, doi: 10.1016/j.jallcom.2009.06.139.
- [32] C. Lupo, F. Eberheim, and D. Schlettwein, “Facile low-temperature synthesis of nickel oxide by an internal combustion reaction for applications in electrochromic devices,” *Journal of Materials Science*, vol. 55, no. 29, pp. 14401–14414, Oct. 2020, doi: 10.1007/s10853-020-04995-8.
- [33] M. Al-Bedairy and H. A. H. Alshamsi, “Environmentally friendly preparation of zinc oxide, study catalytic performance of photodegradation by sunlight for rhodamine B Dye,” *Eurasian Journal of Analytical Chemistry*, vol. 13, no. 6, Dec. 2018, doi: 10.29333/ejac/101785.
- [34] A. H. Ramelan, S. Wahyuningsih, H. Munawaroh, and R. Narayan, “ZnO wide bandgap semiconductors preparation for optoelectronic devices,” *IOP Conference Series: Materials Science and Engineering*, vol. 176, p. 012008, Feb. 2017, doi: 10.1088/1757-899X/176/1/012008.
- [35] A. Singh, D. Mohan, D. Ahlawat, and R. Richa, “Influence of dye loading time and electrolytes constituent’s ratio on the performance of spin coated ZnO photoanode based dye sensitized solar cells,” *Oriental Journal of Chemistry*, vol. 32, no. 2, pp. 1049–1054, Apr. 2016, doi: 10.13005/ojc/320229.
- [36] B. N. Patil and T. C. Taranath, “Limonia acidissima L. leaf mediated synthesis of zinc oxide nanoparticles: a potent tool against Mycobacterium tuberculosis,” *International Journal of Mycobacteriology*, vol. 5, no. 2, pp. 197–204, Jun. 2016, doi: 10.1016/j.ijmyco.2016.03.004.
- [37] M. M. Obeid, H. R. Jappor, K. Al-Marzoki, I. A. Al-Hydary, S. J. Edrees, and M. M. Shukur, “Unraveling the effect of Gd doping on the structural, optical, and magnetic properties of ZnO based diluted magnetic semiconductor nanorods,” *RSC Advances*, vol. 9, no. 57, pp. 33207–33221, 2019, doi: 10.1039/C9RA04750F.
- [38] D. Verma, A. K. Kole, and P. Kumbhakar, “Red shift of the band-edge photoluminescence emission and effects of annealing and capping agent on structural and optical properties of ZnO nanoparticles,” *Journal of Alloys and Compounds*, vol. 625, pp. 122–130, Mar. 2015, doi: 10.1016/j.jallcom.2014.11.102.
- [39] S. Mahato and A. K. Kar, “The effect of annealing on structural, optical and photosensitive properties of electrodeposited cadmium selenide thin films,” *Journal of Science: Advanced Materials and Devices*, vol. 2, no. 2, pp. 165–171, Jun. 2017, doi: 10.1016/j.jsamd.2017.04.001.
- [40] J. A. Kannan and K. Balasubramanian, “Thermally influenced, optical and fluorescence properties of Zinc Oxide nanoparticles for glutathione sensing,” *Applied Physics A*, vol. 126, no. 8, p. 602, Aug. 2020, doi: 10.1007/s00339-020-03780-3.

BIOGRAPHIES OF AUTHORS






Iskandar Dzulkarnain Rummaja     is a graduate research assistant in the Faculty of Electronic and Computer Technology and Engineering at Universiti Teknikal Malaysia Melaka (UTeM) in Melaka, Malaysia. He holds a B.Eng. degree in Electronic Engineering Technology (Industrial Electronics) from the same university and is currently pursuing an M.Sc. in Electronic Engineering at UTeM. His research interests are semiconductors, thin film, solar cells, renewable energy technology, internet of things (IoT), and artificial intelligence (AI). He can be contacted at email: iskandardzulkarnain964@gmail.com.






Nur Afiqah Hani Senin    is a graduate research assistant in the Faculty of Electronic and Computer Technology and Engineering at Universiti Teknikal Malaysia Melaka (UTeM) in Melaka, Malaysia. She holds a B.Eng. degree in Electronic Engineering from the same university and is currently pursuing an M.Sc. in Electronic Engineering at UTeM. Her research interests encompass semiconductor and solar cell technology. She can be contacted at email: m022210004@student.utm.edu.my.






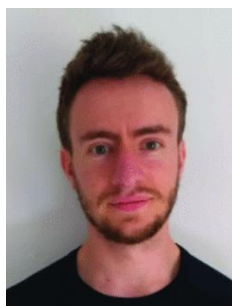
Muhammad Idzdihar Idris    is a senior lecturer in Faculty of Electronic and Computer Technology and Engineering at Universiti Teknikal Malaysia Melaka (UTeM) in Melaka, Malaysia. He received his B.Eng. degree in Electronic System Engineering from Hiroshima University, Japan, M.Sc. in Microelectronics from Universiti Kebangsaan Malaysia (UKM) and Ph.D. in Semiconductor Devices from Newcastle University, United Kingdom in 2010, 2012 and 2018, respectively. His research interests are fabrication and characterization of semiconductor devices: MOSFET, solar cell, and gas sensor. He can be contacted at email: idzdihar@utm.edu.my.






Zarina Baharudin Zamani    is a lecturer in Faculty of Electronic and Computer Technology and Engineering at Universiti Teknikal Malaysia Melaka (UTeM) in Melaka, Malaysia. She received her B.Eng. (Hons) in Electrical from Universiti Teknologi Malaysia (UTM) and M.Sc. in Microelectronics from Universiti Kebangsaan Malaysia (UKM). Her research interests are microelectronics. She can be contacted at email: zarina@utm.edu.my.



Radi Husin Ramlee    is a lecturer in Faculty of Electronic and Computer Technology and Engineering at Universiti Teknikal Malaysia Melaka (UTeM) in Melaka, Malaysia. He received his B.Eng. (Hons) from Universiti Teknologi Malaysia (UTM) and M.Eng. in Electrical from Imperial College London, United Kingdom. His research interests are microelectronics. He can be contacted at email: radihusin@utm.edu.my.



Luke Bradley    is a research associate at the University of Strathclyde within the Rolls Royce UTC group. He attained his Bachelor of Engineering in Electrical and Electronic Engineering from Newcastle University in 2015. Following this, he focused on Cryogenic Power Electronics during his professional tenure and completed his Ph.D. at Newcastle University in 2020. His areas of expertise encompass power electronics and circuits operating at cryogenic temperatures, power device simulations, and the application of microcontroller data logging. He can be contacted at email: luke.bradley@strath.ac.uk.